Use of a combination of in vitro models to investigate the impact of chlorpyrifos and inulin on the intestinal microbiota and the permeability of the intestinal mucosa

Marina Requilé, Duban Ovidio Gonzalez Alvarez, Stéphane Delanaud, Larbi Rhazi, Véronique Bach, Flore Depeint, Hafida Khorsi-Cauet

Use of a combination of *in vitro* models to investigate the impact of chlorpyrifos and inulin on the intestinal microbiota and the permeability of the intestinal mucosa.

Marina Réquilé[1,2], Dubàn Gonzàlez Alvarez [1,2], Stéphane Delanaud [1], Larbi Rhazi [2], Véronique Bach [1], Flore Depeint [2,#] and Hafida Khorsi-Cauet [1,*,#]

Authors' affiliations:

[1] Equipe PERITOX UMR-I01 INERIS, Université Picardie Jules Verne, Amiens, France.

[2] UP 2018.C103 Transformations & Agro-ressources, Institut Polytechnique UniLaSalle, Beauvais, France.

[#] These two senior co-authors contributed equally to the present work.

*Corresponding author: Hafida Khorsi-Cauet. Equipe PERITOX UMR-I101 INERIS; Université Picardie Jules Verne, Centre universitaire de recherche en santé, chemin du Thil, F-80025 Amiens, France. Tel.: +33-322-827-898

E-mail address: hafida.khorsi@u-picardie.fr.

Acknowledgments: The authors thank the French Ministry of Research and Higher Education for funding the present study through MR's postgraduate fellowship. They thank the Picardy Regional Council for providing funding, and also thank David Fraser (Biotech Communication SARL, Ploudalmézeau, France) for copy-editing assistance. The authors also wish to thank Cosucra for kindly providing the inulin used in this project.

Conflict of interests: The authors declare no conflicts of interest.

ABSTRACT

Scope. Dietary exposure to the organophosphorothionate pesticide chlorpyrifos (CPF) has been linked to dysbiosis of the gut microbiota. We therefore sought to investigate whether (i) CPF's impact extends to the intestinal barrier, and (ii) the prebiotic inulin could prevent such an effect.

Methods and results. *In vitro* models mimicking the intestinal environment (the SHIME®) and the intestinal mucosa (Caco-2/TC7 cells) were exposed to CPF. After the SHIME® had been exposed to CPF and/or inulin, we assessed the system's bacterial and metabolic profiles. Extracts from the SHIME®'s colon reactors were then transferred to Caco-2/TC7 cultures, and epithelial barrier integrity and function were assessed. We found that inulin co-treatment partially reversed CPF-induced dysbiosis and increased short-chain fatty acid production in the SHIME®. Furthermore, co-treatment impacted tight junction gene expression and inhibited pro-inflammatory signalling in the Caco-2/TC7 intestinal cell line.

Conclusion. Whereas an isolated *in vitro* assessment of CPF and inulin effects provides useful information on the mechanism of dysbiosis, combining two *in vitro* models increases the *in vivo* relevance.

Keywords: Caco-2/TC7, chlorpyrifos, inulin, dysbiosis, microbiota, SHIME®.

1) Introduction

In 2016, a total of 59,300 metric tons of pesticides were used in France – making the country the third largest user of pesticides worldwide and the prime user in Europe. Some pesticides are considered to be endocrine disrupters; hence, day-to-day exposure is likely to have serious, irreversible effects on organ maturation and development (Lassiter et al. 2008; Joly et al. 2013). Furthermore, some pesticides can cross the placental barrier rapidly, and may therefore affect foetal development. The organophosphorothionate pesticide chlorpyrifos (CPF) has been extensively used in agriculture as a means of controlling insect pests, and is considered to be the most commonly used pesticide worldwide (Harishankar et al. 2013).

Exposure to CPF during early foetal development is known to perturb the gut's environment, permeability and functions (Joly Condette et al. 2015; Reygner et al. 2016b). A pesticide's impact on the digestive tract is of particular interest, since this is the first organ to come into contact with ingested food contaminants. However, there are few data on CPF's mechanisms of action in the digestive tract.

The intestinal microbiota acts as an interface between foodstuff and digestive cells and thus has a role in the intestine's maturation and in digestion. Furthermore, the intestinal microbiota enables the assimilation of nutrients, helps to digest fibre, participates in the synthesis of certain vitamins, and regulates the absorption of fatty acids, calcium and magnesium. It also stimulates immune defences, and acts as a protective barrier against pathogenic microbes and toxins.

The microbiota's composition and diversity change in successive stages from birth onwards, when the neonate passes from the *in utero* compartment (often considered to be sterile) into a microorganism-rich environment. By the age of 3 years, the microbiota's composition and diversity have stabilized and thereafter remain relatively stable throughout life - although some changes have been observed in older adults (Mariat et al. 2009). The microbial environment can nevertheless be disturbed from time to time by factors such as antibiotic treatments, immune system failure, infections, changes in dietary habits, and other changes to the environment. This disturbance is often characterized by a decrease in the numbers of beneficial microorganisms and a simultaneous increase in the numbers of potentially pathogenic microorganisms (Kwok et al. 2014). Like any ecosystem, the intestinal microbiota is usually able to return to its initial state a few weeks after a disturbance; this phenomenon

is referred to as resilience (Antonopoulos et al. 2009). In contrast, persistent instability or imbalance (i.e. intestinal dysbiosis) has often been linked to pathologies such as inflammatory bowel disease (Sokol et al. 2008), obesity, and diabetes (Zhao 2013).

Bacterial translocation corresponds to the passage of viable bacteria from the gastrointestinal flora through the intestinal mucosa's barrier (the lamina propria) to the mesenteric ganglia and then to normally sterile internal organs (such as the spleen and the liver) (Steffen and Berg 1983). Translocation may result from functional alterations in the mucosa and/or increased microbial loads in the intestine.

We have previously reported that chronic, low-dose exposure to CPF causes intestinal dysbiosis in an *in vitro* model of the digestive tract (the Simulator of the Human Intestinal Microbial Ecosystem, SHIME®), with an increase in the numbers of some bacterial strains and a corresponding decrease in others (Joly et al. 2013; Reygner et al. 2016a). However, the SHIME® does not take account of a substance's impact on epithelial cells. Using cultures of Caco-2 cells, Tirelli et al. showed that exposure to 250 µM CPF was associated with tight junction perturbations, the loss of barrier effects, and increased epithelial permeability (Tirelli et al. 2007). However, this Caco-2 cell-based model does not take account of the preliminary metabolism of CPF in the lumen of the digestive tract. Little information is available on CPF-degrading bacteria in the intestinal tract. Some recent studies have evaluated CPF's effects in pure cultures. Treatment with CPF (200 mg/L) was associated with an increase in the counts of four different lactic acid bacteria, which suggests that these strains can tolerate high concentrations of CPF (Cho et al. 2009). Other studies showed that *Streptomyces* spp. and *Pseudomonas* spp. strains were able to tolerate CPF in a mixture of pesticides (Singh et al. 2009; Fuentes et al. 2013). Lastly, another study found that a number of intestinal bacteria had CPF-degrading properties and generated strain-specific metabolites, such as CPF-oxon (also an endogenous metabolite), trichloropyrinidol and diethylphosphate (Harishankar et al. 2013). Although these studies have mechanistic relevance, they involved isolated bacterial cultures. As such, they are not really comparable with our use of a complex *ex vivo* microbiota matrix.

Although a few dynamic, all-in-one in vitro models of the intestinal tract have been developed, they are complex from a technical standpoint (Marzorati et al. 2011). The choice of model also depends on the hypothesis to be tested (von Martels et al. 2017). Here, we decided on the sequential application of the SHIME® and Caco2/TC7

cell cultures. A two-model combination is becoming the gold standard for *in vitro* investigations. We focused on the impacts of the luminal environment and the treatment-modified colonic microbiota on a variety of mucosal parameters, including the tight junction regulation, mucosal permeability to macromolecules, bacterial translocation, and the regulation of epithelial functions.

As mentioned above, a large body of data shows that colonic dysbiosis can be directly treated via dietary intervention. The administration of prebiotics (e.g. dietary fibres such as inulin) might constitute a means of reducing CPF's harmful effects. The impact of inulin on human health has been extensively studied (Roberfroid et al. 2010; Reygner et al. 2016b). Hence, we decided to determine whether or not CPF's effects on selective bacterial growth and bacterial metabolite levels could be reversed by introducing the prebiotic inulin into the diet. Prebiotics are non-digestible food ingredients that benefit the host by acting as a substrate for certain bacteria in the digestive tract. Interactions and competition between beneficial bacteria and potentially pathogenic bacteria can positively or negatively influence the microbiota. Indeed, the growth of beneficial bacteria (*Bifidobacterium* spp. and *Lactobacillus* spp.) can prevent potentially pathogenic bacteria from colonizing the digestive tract by modifying the pH or stimulating the production and release of short-chain fatty acids (SCFAs) (Roberfroid et al. 2010).

The objective of the present study was to better understand CPF's impact on the intestinal luminal ecosystem and the epithelium *in vitro*. We therefore combined two systems, one mimicking the physical-chemical conditions in the lumen and the other mimicking a working epithelial mucosa. The impact on the lumen was assessed by measuring selected bacterial populations and bacterial metabolites, whereas the impact on the epithelium was assessed by measuring the expression of tight junction proteins. The study secondary objective was to investigate the putative protective effect of a prebiotic (inulin) on these parameters.

2) Materials and Methods

The overall experimental design is summarized in Figure 1.

Chemicals

Chlorpyrifos (purity: 99.8%) was purchased from LGC Standards (Molsheim, France). The stock solution (10 mg/mL) was prepared in vegetable oil. Next, 3.5 mL of the stock solution were mixed with 96.5 mL of the primary feed (Molly et al. 1993b), giving a 0.35 mg/mL working solution (stored at 4°C). 50 g of inulin (kindly provided by Cosucra, Warcoing, Belgium) were added to 1 L of primary feed, mixed for 30 min, and stored at 4 °C.

The SHIME® model

The SHIME® is a dynamic *in vitro* model of the human microbial ecosystem (Molly et al. 1993b), and has been described in detail by Joly et al (Joly et al. 2013). Six double-jacketed reactors are connected in series via peristaltic pumps. The reactors respectively mimic the stomach, two segments of the small intestine (the duodenum/jejunum and the ileum/cecum), and the ascending, transverse, and descending segments of the colon. Each of the colon segments was connected to a pH probe, which recorded the change of pH in the medium. Twice a day, the pH was adjusted to the physiological value or range (Table 1). The residence time in each reactor is determined by its working volume, and the total transit time is 86 hours. The compositions of the SHIME®'s feed and pancreatic juice have been described elsewhere (Molly et al. 1993a; De Boever et al. 2000). To mimic feeding patterns, 200 mL of primary feed were added to reactor 1 every 8 hours.

Treatment

The colon reactors were inoculated with a mixture of faecal microbiota from five healthy adult volunteers (including males and females), none of whom had suffered from gastrointestinal diseases or taken antibiotics in the previous six months (Joly et al. 2013). In view of the system's technical parameters, no more than two conditions can be tested in parallel. To ensure the absence of selective degradation of the microbiota during storage, samples were used fresh for each experiment. However, samples from the same set of volunteers were used to minimize the variability of the microbial profiles. The *in vitro* environment had stabilized after 14 days, as proven by stable pH fluctuations within the physiological range (Table 1) and a stable redox potential. Day 0 (D0) was defined as the untreated control value. Samples were collected from the different reactors on three non-consecutive days, to increase the number of replicates. Immediately after collection of the final untreated samples, 10 mL of the CPF solution (3.5 mg) and 200 mL of primary feed containing the inulin (10 g) were

injected daily into reactor 1 for 30 days. Only the first of the day's three meals contained the treatments. Fifteen and 30 days after the initiation of treatment (i.e. on D15 and D30), samples were collected from reactors 4 to 6 (representing the ascending, transverse and descending colon, respectively) and used immediately for microbiological studies or stored at -20 °C prior to analysis. Again, with a view to increasing the number of replicates, triplicate samples were collected on non-consecutive days. We also performed CPF-only and inulin-only SHIME® treatments.

Microbiological evaluation

Serial dilutions (1/10) of fresh samples from reactors 4 to 6 were prepared in Ringer solution (Oxoid, Basingstoke, England). The microorganisms were identified using standard microbiological techniques and various non-selective, selective, semi-selective and indicator bacterial growth media (Joly et al. 2013). All anaerobic plates were incubated in a Bactron anaerobic chamber (Sheldon Manufacturing, Inc., Cornelius, OR, USA) for 5 days. Isolated colonies grown on Petri dishes were counted using an automatic colony counter (Scan® 500, Interscience, St Nom la Bretèche, France) and expressed in log(CFU)/mL. Although bacterial cultures detect (by definition) only culturable, viable strains, these are the ones of interest; our ultimate objective is to investigate bacterial translocation through the epithelial layer and to the basal compartment.

Short-chain fatty acids

Fermentation slurries were centrifuged at 14,000 g for 10 min, and the supernatants were filter-sterilized (VWR International, Strasbourg, France). 100 µL of internal standard and 50 µL of sulfuric acid were added to 900 µL of supernatant. The SCFA content was determined as described elsewhere (Lecerf et al. 2012) using a Focus GC gas chromatograph (Thermo Scientific, Illkirch, France) equipped with a flame ionization detector and a gas chromatography column (length: 30 m; inner diameter: 25 mm; film: 1 µm), with H_2 as the carrier gas at a flow rate of 1 mL/min. The different SCFAs were identified according to the elution peaks' respective retention times, and then quantified by comparison with standard curves.

Caco-2/TC7 cell culture

The Caco-2/TC7 intestinal cell line was kindly provided by Dr M. Rousset (INSERM U178, Villejuif, France). The cells were cultured in Dulbecco's Modified Eagle Medium (DMEM) supplemented with 10% heat-inactivated foetal bovine serum, 1% non-essential amino acids (100 X) and 100 units/mL penicillin–streptomycin. All these reagents were purchased from Gibco (Fisher Scientific SAS, Illkirch, France).

Isolated cells were seeded directly onto polycarbonate inserts in tissue-culture-treated 6-well plates (diameter: 24 mm; pore size: 1 µm; Fisher Scientific SAS) at a density of 250,000 cells/insert. The medium was refreshed every other day for 21 days; at this time point, the epithelial cells had differentiated fully and formed a tight, functional monolayer (as assessed by the transepithelial electrical resistance [TEER]).

Treatment

The treatment was initiated at 21–23 days post-seeding. Frozen samples from the SHIME® experiment were thawed and either used as such or as the supernatant (SHIME® luminal medium) after centrifugation at 5000 rpm for 5 min and filtration through a 0.2 µm pore membrane). Each of the triplicate samples collected from reactor 4 at D0, D15 and D30 was added instead of culture medium to a separate well (n=3). We also included samples from CPF-only and inulin only SHIME® treatments in this experiment. Cells were exposed to the various treatments for 6 or 24 hours.

Epithelial layer integrity

The integrity of a monolayer of differentiated Caco-2/TC7 cells growing on inserts was monitored by measuring the TEER (Tirelli et al. 2007). After a 15 min stabilization period, the TEER was recorded at room temperature using chop-stick electrodes (Millicell®ERS-2, Millipore, Molsheim, France) and expressed in Ω x cm^2, according to the following equation: TEER = (Ω cell monolayer - Ω cell–free filter) x filter surface area

Genetic expression

All reagents and working kits were purchased from Qiagen SA (Courtaboeuf, France). Caco 2/TC7 cells were collected in RNAprotect Cell Reagent prior to storage. After centrifugation (14,000 g, 1 min), total RNA was extracted from the cell pellet using an RNeasy® Mini Kit, according to the manufacturer's instructions. The mRNA content in the flow-through was determined spectrophotometrically using a NanoDrop 2000 system

(Thermo Scientific, Illkirch, France). Complementary DNA (cDNA) was generated by reverse transcription of 200 ng mRNA using a QuantiTect® Reverse Transcription kit, according to the manufacturer's instructions. The real-time quantitative polymerase chain reaction (RT-PCR) was performed on 5 µL of cDNA (diluted 1/10 in RNase-free water), 1 µL of primers (Primerdesign Ltd, Southampton, UK), 4 µL of RNase-free water and 10 µL of QuantiFast® SYBR® Green PCR Master Mix in a total of 20µL per sample (in triplicate). The target genes and corresponding primers are listed in supplementary table 1. Following activation of the HotStart Taq DNA polymerase (95 °C, 5 min), 40 cycles of amplification (denaturation at 95 °C, 10 sec followed by annealing/extension at 60 °C, 30 sec) were performed with fluorescence detection at the end of each extension step. This was followed by a melting curve analysis (from 60 °C to 95 °C) for quality control of the amplicons. Relative expression was calculated with regard to untreated cells, and both *GAPDH* and *ATP5B* were used as reference genes.

Secretion of an inflammatory marker

The secretion of interleukin-8 (IL-8) into the apical medium was studied by assaying 50 µL samples with a Bio-Plex Pro™ Human Cytokine IL-8 Assay Kit (Bio-Rad Laboratories Inc., Marnes-la-Coquette, France), according to the manufacturer's instructions. The plate was read using flow cytometry (MACS QUANT® Analyser, Miltenyi biotech, Bergisch Gladbach, Germany). The IL-8 was then quantified by reference to a standard curve.

Statistical analyses

Data were expressed as the mean ± standard deviation (SD). The various experimental conditions were compared in a one-way analysis of variance. All statistical analyses were performed using StatView software (version 5.0, Abacus Concepts Inc., Berkeley, CA, USA). The threshold for statistical significance was set to $p < 0.05$.

3) Results and Discussion

Impact of CPF and inulin co-treatment on the bacterial intestinal environment, as assessed with the SHIME® model

The data presented here relate to reactor 4, since (i) the ascending colon is where most of the inulin is metabolized in vivo, and (ii) the intestinal cells were treated with samples taken from this reactor (*in vivo*, the ascending colon is the closest part of the colon to the small intestine's mucosa). In contrast to the marked dysbiosis observed previously at a dose of 1 mg/d *in vitro* (Joly et al. 2013; Reygner et al. 2016a) or at the equivalent dose of 3.5 mg/d *in vivo* (Reygner et al. 2016b), exposure of the SHIME® to the dose of 3.5 mg/d used here significantly reduced the *Lactobacillus* and the *Bifidobacterium* counts (Figure 2C and 2D), while counts of other selected bacteria (including pathobionts like *Enterobacteriacea* and *Enterococcus*) were not significantly modified (figure 2A and 2B). Inulin increased the *Lactobacillus* and *Bifidobacterium* counts but also reduced the *Enterococcus* count and the *Enterobacteriacea* counts; however, none of these changes were statistically significant. The combination of CPF and inulin significantly reduced the *Enterococcus* count, while the *Bifidobacterium* and *Lactobacillus* counts were not significantly affected. The *Enterobacteriacea* count decreased over time but the change was not statistically significant. The overall effect (as summarised in Figure 2) partially prevented an increase in the pathobionts count and was associated with a non-significant decrease in the numbers of lactic acid bacteria. Molecular profiling of the whole microbiota would probably provide more accurate information on the combined effects of CPF and inulin, since some of the affected bacteria might not have been cultured in our tests.

There are only limited data on the interactions between CPF and the human microbiota. However, *in vivo* and *in vitro* experiments (Joly et al. 2013; Joly Condette et al. 2015; Reygner et al. 2016b, a) demonstrated that a 30-day period of CPF treatment was associated with increase in the numbers of potentially pathogenic microbiota and a decrease in the numbers of beneficial microbiota in all segments of the colon. The literature data indicate that CPF exposure in the rat is associated with higher *Staphylococcus spp*. counts in all segments of the digestive tract (Joly Condette et al. 2015). In contrast to the negative impact of CPF, van de Wiele et al. (van de Wiele et

al. 2004; van de Wiele et al. 2007) and others (Allsopp et al. 2013; Sivieri et al. 2014) have confirmed the prebiotic effects of chicory inulin on *Bifidobacterium* and *Lactobacillus* in all segments of the colon. To the best of our knowledge, there are no previous reports of CPF and inulin co-treatment in the SHIME® or in similar models; hence, we can only refer to our own data to discuss inulin's role with respect to CPF. The data from our previous experiments in the rat at the same CPF concentration (3.5 mg/day) indicate that *in vitro* and *in vivo* co-treatments with CPF and inulin have similar effects on bacterial populations (Reygner et al. 2016b).

Total SCFA levels increased under all three treatment conditions, although the increase was only statistically significant with the CPF+inulin mixture; this was probably due to the small number of replicates in each condition (Figure 3). However, the profiles of individual SCFAs differed as a function of the treatment. The presence of CPF alone increased the acetic acid content (from 18.49 ± 2.91 µmol/mL at D0 to 25.07 ± 7.68 µmol/mL at D30), the presence of inulin increased the propionic and butyric acid levels (from 0.98 ± 0.60 µmol/mL at D15 to 3.81 ± 0.39 µmol/mL at D30 for proprionate, and from 0.62 ± 0.40 µmol/mL at D15 to 0.91 ± 0.66 µmol/mL at D30 for butyrate), and the CPF+inulin mixture increased the propionic acid level (from 7.57 ± 0.60 µmol/mL at D0 to 15.36 ± 2.88 µmol/mL at D30). It is generally considered that the ratios between the three main SCFAs (Figure 3) are more meaningful than the absolute concentrations. These values gave a slightly different picture. CPF alone did not change the ratios - suggesting that all the bacteria responsible for saccharolytic hydrolysis are metabolically modulated by the pesticide in a similar manner. In the prebiotic group, we did not observe the shift in propionate and butyrate production (an increase in total, propionic and butyric acids in all segments of the colon) observed in a number of *in vitro* SHIME® experiments (van de Wiele et al. 2004) following inulin treatment for 3 weeks. We even observed an unexpected fall in propionate's contribution at D15, although we could not link it to specific bacterial modulations. The CPF+inulin mixture was associated with a large, statistically significant decrease in the acetic acid ratio in R4 and a significant increase in the propionic acid ratio. The butyric acid ratio was not affected (Figure 3C). Overall, increased SCFA synthesis creates an acidic environment in the colon; *in vivo*, this protects against pathogens such as *Enterococcus* and the *Enterobacteriaceae*, as shown by our microbial measurements in the CPF+inulin condition. The pH was measured daily as part of the system check; a decrease in pH was observed as early as day 7 (data not shown). However, the system set-up requires the pH to be maintained within a predefined range, and so the pH was adjusted twice a day - preventing further acidification. Our observation of elevated SCFA release constitutes

additional evidence of inulin's ability to relieve (at least in part) the damage caused by exposure to CPF. The increase in SCFA levels may appear to be inconsistent with the transient increase in numbers of *Staphylococcus* measured at D15 (data not shown) time but is in line with the inhibition of *Enterococcus* as early as D15. Further investigations at earlier time points might provide a better understanding of the relationship (if any) between bacterial species and saccharolytic metabolites. Furthermore, SCFAs constitute an important energy source for colonocytes, and also influence colonic function by stimulating sodium and water absorption and modulating motility (Topping and Clifton 2001). This is important when considering the impact of SHIME® extracts on intestinal cells and the latter's function.

Impact of CPF and inulin on Caco-2/TC7 cells following digestion in the SHIME®.

In the CPF-only, inulin-only and CPF+inulin experiments in the SHIME®, samples from reactor 4 were tested on Caco-2/TC7 cells.

Exposure to SHIME® extracts led to a fall in the TEER over time. Baseline (D0) TEER values were above that of culture medium for the CPF and inulin treatments but not the mix. While this is likely due to the more complex molecular composition of the media, it remains unclear why the three conditions are not equivalent at baseline. Compared to their D0 control, total (unfiltered) SHIME® extracts led to a loss of tissue integrity as early as 2 hours, and so were not used further. Although filtered SHIME® extracts also induced a drop in the TEER (supplementary table 2), the value remained significantly close to that of the control value (D0 untreated SHIME® medium) for up to 8 hours. The time-dependent drop in TEER suggests that the permeability of the Caco-2/TC7 monolayer increases quickly following exposure to SHIME® extracts. Observation of the wells showed that at 24 hours, the cell layer had detached from the membrane surface. Following further tests, we determined that a 1:5 dilution of the SHIME® sample did not affect the stability of the epithelial layer, as measured by the TEER and dextran-FITC diffusion to the basal compartment (data not shown). However, the data presented here come from the exposure of undiluted SHIME® extracts. Given that the TEER dropped quickly, we examined the functional status of treated cells at 6 hours. We are aware that these data may not be fully representative of physiological exposure.

Cells exposed to SHIME® samples showed no variations in the expression levels of structural genes associated with cell differentiation and epithelial function (*ACTB, VIL1, ALPI, SI*) for D0 samples (Table 2), suggesting that the epithelium remained functional for these reference conditions. At D15, cells exposed to CPF-treated extracts had significantly lower expression levels of all tested genes (overall decrease: 30%), with the exception of the differentiation genes *ALPI* and *SI* (no variation). Inulin-treated extracts did not change overall expression levels, even though *ALPI* was increased at D15, whereas cells exposed to the CPF-inulin SHIME® samples showed a large, time-dependant and significant increase in expression of the structural gene *VIL1* (2-fold) and of the tight junction genes *CDH1* (2-fold), *OCLN* (4-fold) and *TJP1* (5-fold), as well as differentiation genes *ALPI* and *SI* relative to SHIME® samples collected on D0 (controls). In summary, we found that CPF alone tended to inhibit the expression of tight junction and structural genes, whereas inulin and CPF/inulin co-treatment tended to increase expression. Altogether this suggests that the pesticide disrupted the tight junctions while the mix led to strengthening of this activity. With regard to genes coding for bacterial and luminal receptors, the expression level of *TLR4* rose strongly and significantly at D30 (8-fold) with CPF+inulin but not with CPF alone or inulin alone, suggesting that a specific luminal environment was created by changes in bacterial populations other than those measured here.

To the best of our knowledge, similar *in vitro* experiments have not been reported in the literature. Hence, we can only relate the present *in vitro* data to our previous *in vivo* findings. The increase in *TJP1* and *OCLN* expression might compensate for CPF-induced leakage through the intermembrane space observed *in vivo* (Joly Condette et al. 2015). The strong increase in *TJP1* gene expression may be a sign of increased production of the encoded tight junction protein zonula occludens-1 (González-Mariscal et al. 2014). We found that samples exposed to CPF alone for 30 days were associated with downregulated expression of the *CDH1* gene (coding for the transmembrane glycoprotein E-cadherin). Several studies have shown that low *CDH1* expression may be a risk factor for gastric cancer (Al-Moundhri et al. 2010). E-cadherin has an important role not only in regulating the morphogenesis of normal and neoplastic tissues but also in tumour invasion and metastasis (Gao et al. 2008). With regard to genes encoding functional proteins, we observed that the expression levels of *SI* and *ALPI* were increased by CPF alone and CPF+inulin but not by inulin alone. Overexpression of *ALPI* may be associated with a recovery from an initial toxic episode because alkaline phosphatase is known to be involved in reducing inflammatory responses (Lallès 2014); this might be related to the early (D15) increase in the numbers of

Staphylococcus. Furthermore, the enzyme has been linked to the expression of Toll-like receptor (TLR) 4 and the inhibition of IL-8 secretion (Chen and Ouyang 2010). However, recent studies have shown that contact between inulin and gut epithelia cells can modify epithelial tight junction integrity and signals related to the immune response (Vogt et al. 2015). Lastly, Toll-like receptors are involved in bacterial sensing, and have an important role in controlling the homeostasis of the intestinal epithelium. Changes in TLR gene expression may be indicative of an imbalance in the microbiota and disturbance of the intestinal immune system (Rakoff-Nahoum et al. 2004). The increase in TLR gene expression after exposure to CPF+inulin co-treatment may be related to the modulation of bacterial loads in general and that of the *Enterobacteriaceae* in particular (Lu et al. 2008). It is not clear whether gene expression levels and bacterial counts were in our experimental setting. Changes in bacterial populations other than those measured here might have modulated gene expression in the Caco-2/TC7 cells.

The release of IL-8 increased in a time-dependant manner in the CPF-only condition (Figure 4; $p < 0.05$ vs. D0) but remained low and stable for the inulin-only treatment and CPF-inulin conditions. These observations suggest that a proinflammatory signal is triggered by the pesticide but completely inhibited by the prebiotic.

These data are consistent with (i) our experiments on CPF-treated caco-2/TC7 cells (supplementary table 3), in which CPF induced IL8 secretion in a dose-dependent manner, (ii) modulation of the bacterial environment by the pesticide and the prebiotic (as measured in the SHIME® reactors), and (iii) the known anti-inflammatory role of probiotic bacteria, including *Bifidobacterium* strains (Park Ms et al. 2007; Candela et al. 2008; Wang et al. 2011). Based on CPF's molecular weight and its dilution in the SHIME® solutions, we estimate that the concentration of CPF in the colonic reactors is between 10 and 50 µM. At these concentrations, CPF in culture medium did not induce IL8 release into the luminal compartment. We thus hypothesize that CPF itself and CPF-induced factors in the SHIME® content may have synergistically induced an inflammatory response. Co-treatment with inulin and CPF had a marked impact by preventing the CPF-induced decrease in *Bifidobacterium* spp and modulating SCFA production in the colon reactors. As mentioned above, there are very few reports on CPF's effects on bacterial populations *in vivo* or *in vitro* (Joly et al. 2013; Joly Condette et al. 2015; Reygner et al. 2016b, a). Most of the previous work used a CPF dose of 1 mg/d, which resulted in more severe dysbiosis (as measured by larger log differences at the end of the treatment period) than the higher concentration of 3.5 mg/d

studied here. We suggest that some of the potentially discriminant bacterial responses to CPF observed at the lower concentration may have been saturated at the higher concentration - leading to changes that are independent of the bacterial species measured herein. Nevertheless, we observed a clear association between (i) luminal variables in the SHIME® and (ii) epithelial function, as measured in Caco-2/TC7 cell layers.

The relevance of combined *in vitro* models

Several studies have shown that the SHIME® is a relevant model for evaluating compounds such as probiotics/prebiotics (Terpend et al. 2013; Chaikham and Apichartsrangkoon 2014), drug candidates (Sousa et al. 2008), plant extracts (Muñoz-González et al. 2015), and toxics (Joly et al. 2013). However, this model also presents certain limitations, such as the absence of (i) bacterial adhesion to the gut epithelium, (ii) microbiota-host crosstalk, and (iii) immune feedback and regulation (Mainville et al. 2005). Some of these limitations can be circumvented by performing additional studies with Caco-2/TC7 cells. Under specific conditions, Caco-2/TC7 cells can form a simple, functional intestinal epithelium in which polarized cells have tight junctions and a brush border on the apical side. Furthermore, the Caco-2/TC7 monolayer presents a high TEER and can produce cytokines (such as IL-6, IL-8, TNFα, and IL-15) (Sambuy et al. 2005; Verhoeckx et al. 2015). Moreover, the Caco-2/TC7 monolayer's permeability coefficients *in vitro* are strongly correlated with absorption data measured *in vivo* in humans (Verhoeckx et al. 2015).

By combining the SHIME® and Caco-2/TC7 models, it is possible to gain a better understanding of how different food components alter (and are altered by) the gastrointestinal environment and microbial populations before they reach the intestinal mucosa. The SHIME®-Caco-2/TC7 combination is not the first two-model system to have been reported. However, previously described combined models were used to investigate prebiotic activity with regard to mucosal health rather than a prebiotic's ability to protect the mucosa against an environmental disruptor.

In the present and previous studies, we found that CPF induces dysbiosis and a metabolic imbalance in the intestinal environment. While further analyses are required to fully characterize CPF's impact, it appears that one mechanism involves the inhibition of the growth and metabolism of lactic acid bacteria. These harmful effects were prevented (at least in part) by co-treatment with inulin, thanks to the recovery of health-promoting strains

and the production of saccharolytic metabolites. We were not able to draw firm conclusions about barrier function parameters. It is nevertheless clear that CPF affected the activity of the mucosal barrier and the release of the chemokine IL-8, which might potentiate inflammation processes through the recruitment of immune effectors. Lastly, CPF/inulin co-treatment was associated with an increase in TLR gene expression. Notably, this increase in expression was concomitant with the bacterial changes measured in the corresponding SHIME® samples.

However, prolonged apical exposure to SHIME® extracts (even in the absence of CPF) appeared to disrupt the Caco-2/TC7 monolayer. It might be of value to adjust the experimental set-up by (i) diluting the SHIME® extract in culture medium, and (ii) determining the optimal time range for measuring effects on gene expression and physiological parameters. Lastly, with a view to modelling the complexity of mucosal tissue more accurately, the combination of the SHIME® model and the Caco-2/TC7 model could be developed further by the inclusion of mucus-producing or immune cells. Even in its current state, the combination of these two *in vitro* models seems to be a relevant, ethically acceptable alternative to animal experiments.

Abbreviations: CPF, chlorpyriphos; SHIME®, Simulator of the Human Intestinal Microbial Ecosystem; cDNA: complementary DNA; D, day; TLR, Toll-like receptor; TEER, transepithelial electrical resistance.

Authors' contributions: HKC, FD and VB designed the research programme; HKC and FD conceived and designed the SHIME® and cell-based experiments, respectively; DOGA, MR and LR performed the experiments and assays; DOGA, MR and VB analyzed the data; SD contributed materials and analytical tools for the SHIME®; MR, DOGA, FD and HKC wrote, evaluated and revised the manuscript. All authors read and approved the final manuscript.

4) References

Allsopp P, Possemiers S, Campbell D, et al (2013) An exploratory study into the putative prebiotic activity of fructans isolated from Agave angustifolia and the associated anticancer activity. Anaerobe 22:38–44. doi: 10.1016/j.anaerobe.2013.05.006

Al-Moundhri MS, Al-Khanbashi M, Al-Kindi M, et al (2010) Association of E-cadherin (CDH1) gene polymorphisms and gastric cancer risk. World J Gastroenterol 16:3432–3436

Antonopoulos DA, Huse SM, Morrison HG, et al (2009) Reproducible community dynamics of the gastrointestinal microbiota following antibiotic perturbation. Infect Immun 77:2367–2375. doi: 10.1128/IAI.01520-08

Candela M, Perna F, Carnevali P, et al (2008) Interaction of probiotic Lactobacillus and Bifidobacterium strains with human intestinal epithelial cells: adhesion properties, competition against enteropathogens and modulation of IL-8 production. Int J Food Microbiol 125:286–292. doi: 10.1016/j.ijfoodmicro.2008.04.012

Chaikham P, Apichartsrangkoon A (2014) Effects of encapsulated Lactobacillus acidophilus along with pasteurized longan juice on the colon microbiota residing in a dynamic simulator of the human intestinal microbial ecosystem. Appl Microbiol Biotechnol 98:485–495. doi: 10.1007/s00253-013-4763-7

Chen X, Ouyang Q (2010) [Study on the molecular expression and regulation of toll pathway in HT-29 cells]. Sichuan Da Xue Xue Bao Yi Xue Ban 41:581–585

Cho KM, Math RK, Islam SMA, et al (2009) Biodegradation of Chlorpyrifos by Lactic Acid Bacteria during Kimchi Fermentation. J Agric Food Chem 57:1882–1889. doi: 10.1021/jf803649z

De Boever P, Deplancke B, Verstraete W (2000) Fermentation by gut microbiota cultured in a simulator of the human intestinal microbial ecosystem is improved by supplementing a soygerm powder. J Nutr 130:2599–2606

de Wiele TV, Boon N, Possemiers S, et al (2004) Prebiotic effects of chicory inulin in the simulator of the human intestinal microbial ecosystem. FEMS Microbiol Ecol 51:143–153. doi: 10.1016/j.femsec.2004.07.014

Fuentes MS, Briceño GE, Saez JM, et al (2013) Enhanced Removal of a Pesticides Mixture by Single Cultures and Consortia of Free and Immobilized Streptomyces Strains. In: BioMed Res. Int. https://www.hindawi.com/journals/bmri/2013/392573/abs/. Accessed 21 Feb 2018

Gao L, Nieters A, Brenner H (2008) Meta-analysis: tumour invasion-related genetic polymorphisms and gastric cancer susceptibility. Aliment Pharmacol Ther 28:565–573. doi: 10.1111/j.1365-2036.2008.03760.x

González-Mariscal L, Domínguez-Calderón A, Raya-Sandino A, et al (2014) Tight junctions and the regulation of gene expression. Semin Cell Dev Biol 36:213–223. doi: 10.1016/j.semcdb.2014.08.009

Harishankar MK, Sasikala C, Ramya M (2013) Efficiency of the intestinal bacteria in the degradation of the toxic pesticide, chlorpyrifos. 3 Biotech 3:137–142. doi: 10.1007/s13205-012-0078-0

Joly C, Gay-Quéheillard J, Léké A, et al (2013) Impact of chronic exposure to low doses of chlorpyrifos on the intestinal microbiota in the Simulator of the Human Intestinal Microbial Ecosystem (SHIME®) and in the rat. Environ Sci Pollut Res 20:2726–2734. doi: 10.1007/s11356-012-1283-4

Joly Condette C, Bach V, Mayeur C, et al (2015) Chlorpyrifos Exposure During Perinatal Period Affects Intestinal Microbiota Associated With Delay of Maturation of Digestive Tract in Rats. J Pediatr Gastroenterol Nutr 61:30–40. doi: 10.1097/MPG.0000000000000734

Kwok LY, Zhang J, Guo Z, et al (2014) Characterization of fecal microbiota across seven Chinese ethnic groups by quantitative polymerase chain reaction. PLoS ONE 9:1–11. doi: 10.1371/journal.pone.0093631

Lallès J-P (2014) Intestinal alkaline phosphatase: novel functions and protective effects. Nutr Rev 72:82–94. doi: 10.1111/nure.12082

Lassiter TL, Ryde IT, Mackillop EA, et al (2008) Exposure of neonatal rats to parathion elicits sex-selective reprogramming of metabolism and alters the response to a high-fat diet in adulthood. Environ Health Perspect 116:1456–1462. doi: 10.1289/ehp.11673

Lecerf J-M, Dépeint F, Clerc E, et al (2012) Xylo-oligosaccharide (XOS) in combination with inulin modulates both the intestinal environment and immune status in healthy subjects, while XOS alone only shows prebiotic properties. Br J Nutr 108:1847–1858

Lu Y-C, Yeh W-C, Ohashi PS (2008) LPS/TLR4 signal transduction pathway. Cytokine 42:145–151. doi: 10.1016/j.cyto.2008.01.006

Mainville I, Arcand Y, Farnworth ER (2005) A dynamic model that simulates the human upper gastrointestinal tract for the study of probiotics. Int J Food Microbiol 99:287–296. doi: 10.1016/j.ijfoodmicro.2004.08.020

Mariat D, Firmesse O, Levenez F, et al (2009) The Firmicutes/Bacteroidetes ratio of the human microbiota changes with age. BMC Microbiol 9:123. doi: 10.1186/1471-2180-9-123

Marzorati M, Abbeele PV den, Possemiers S, et al (2011) Studying the host-microbiota interaction in the human gastrointestinal tract: basic concepts and in vitro approaches. Ann Microbiol 61:709–715. doi: 10.1007/s13213-011-0242-5

Molly K, van de Woestyne M, Verstraete W (1993a) Development of a 5-step multi-chamber reactor as a simulation of the human intestinal microbial ecosystem. Appl Microbiol Biotechnol 39:254–258. doi: 10.1007/BF00228615

Molly K, Vande Woestyne M, Verstraete W (1993b) Development of a 5-step multi-chamber reactor as a simulation of the human intestinal microbial ecosystem. Appl Microbiol Biotechnol 39:254–258

Muñoz-González C, Cueva C, Ángeles Pozo-Bayón M, Victoria Moreno-Arribas M (2015) Ability of human oral microbiota to produce wine odorant aglycones from odourless grape glycosidic aroma precursors. Food Chem 187:112–119. doi: 10.1016/j.foodchem.2015.04.068

Park Ms, Kim Mj, Ji Ge (2007) Assessment of lipopolysaccharide-binding activity of Bifidobacterium and its relationship with cell surface hydrophobicity, autoaggregation, and inhibition of interleukin-8 production. J Microbiol Biotechnol 17:1120–1126

Rakoff-Nahoum S, Paglino J, Eslami-Varzaneh F, et al (2004) Recognition of commensal microflora by toll-like receptors is required for intestinal homeostasis. Cell 118:229–241. doi: 10.1016/j.cell.2004.07.002

Reygner J, Joly Condette C, Bruneau A, et al (2016a) Changes in Composition and Function of Human Intestinal Microbiota Exposed to Chlorpyrifos in Oil as Assessed by the SHIME(®) Model. Int J Environ Res Public Health 13:. doi: 10.3390/ijerph13111088

Reygner J, Lichtenberger L, Elmhiri G, et al (2016b) Inulin Supplementation Lowered the Metabolic Defects of Prolonged Exposure to Chlorpyrifos from Gestation to Young Adult Stage in Offspring Rats. PloS One 11:e0164614. doi: 10.1371/journal.pone.0164614

Roberfroid M, Gibson GR, Hoyles L, et al (2010) Prebiotic effects: metabolic and health benefits. Br J Nutr 104 Suppl 2:S1-63. doi: 10.1017/S0007114510003363

Sambuy Y, De Angelis I, Ranaldi G, et al (2005) The Caco-2 cell line as a model of the intestinal barrier: influence of cell and culture-related factors on Caco-2 cell functional characteristics. Cell Biol Toxicol 21:1–26. doi: 10.1007/s10565-005-0085-6

Singh P b., Sharma S, Saini H s., Chadha B s. (2009) Biosurfactant production by Pseudomonas sp. and its role in aqueous phase partitioning and biodegradation of chlorpyrifos. Lett Appl Microbiol 49:378–383. doi: 10.1111/j.1472-765X.2009.02672.x

Sivieri K, Morales MLV, Saad SMI, et al (2014) Prebiotic effect of fructooligosaccharide in the simulator of the human intestinal microbial ecosystem (SHIME® model). J Med Food 17:894–901. doi: 10.1089/jmf.2013.0092

Sokol H, Pigneur B, Watterlot L, et al (2008) Faecalibacterium prausnitzii is an anti-inflammatory commensal bacterium identified by gut microbiota analysis of Crohn disease patients. Proc Natl Acad Sci U S A 105:16731–16736. doi: 10.1073/pnas.0804812105

Sousa T, Paterson R, Moore V, et al (2008) The gastrointestinal microbiota as a site for the biotransformation of drugs. Int J Pharm 363:1–25. doi: 10.1016/j.ijpharm.2008.07.009

Steffen EK, Berg RD (1983) Relationship between cecal population levels of indigenous bacteria and translocation to the mesenteric lymph nodes. Infect Immun 39:1252–1259

Terpend K, Possemiers S, Daguet D, Marzorati M (2013) Arabinogalactan and fructo-oligosaccharides have a different fermentation profile in the Simulator of the Human Intestinal Microbial Ecosystem (SHIME ®). Environ Microbiol Rep 5:595–603. doi: 10.1111/1758-2229.12056

Tirelli V, Catone T, Turco L, et al (2007) Effects of the pesticide clorpyrifos on an in vitro model of intestinal barrier. Toxicol In Vitro 21:308–313. doi: 10.1016/j.tiv.2006.08.015

Topping DL, Clifton PM (2001) Short-chain fatty acids and human colonic function: roles of resistant starch and nonstarch polysaccharides. Physiol Rev 81:1031–1064

van de Wiele T, Boon N, Possemiers S, et al (2007) Inulin-type fructans of longer degree of polymerization exert more pronounced in vitro prebiotic effects. J Appl Microbiol 102:452–460. doi: 10.1111/j.1365-2672.2006.03084.x

Verhoeckx KCM, Vissers YM, Baumert JL, et al (2015) Food processing and allergenicity. Food Chem Toxicol Int J Publ Br Ind Biol Res Assoc 80:223–240. doi: 10.1016/j.fct.2015.03.005

Vogt L, Meyer D, Pullens G, et al (2015) Immunological properties of inulin-type fructans. Crit Rev Food Sci Nutr 55:414–436. doi: 10.1080/10408398.2012.656772

von Martels JZH, Sadaghian Sadabad M, Bourgonje AR, et al (2017) The role of gut microbiota in health and disease: In vitro modeling of host-microbe interactions at the aerobe-anaerobe interphase of the human gut. Anaerobe 44:3–12. doi: 10.1016/j.anaerobe.2017.01.001

Wang Z, Wang J, Cheng Y, et al (2011) Secreted factors from Bifidobacterium animalis subsp. lactis inhibit NF-κB-mediated interleukin-8 gene expression in Caco-2 cells. Appl Environ Microbiol 77:8171–8174. doi: 10.1128/AEM.06145-11

Zhao L (2013) The gut microbiota and obesity: from correlation to causality. Nat Rev Microbiol 11:639–647. doi: 10.1038/nrmicro3089

Figure captions.

Figure 1: Schematic representation of the experimental set-up and design.

Figure 2: Changes over time in bacterial populations in reactor 4, following co-treatment with CPF and inulin.

After 14 days of stabilization, the SHIME® was exposed to daily treatment with CPF (3.5 mg) and/or inulin (10 g). Three samples were collected every other day before treatment (D0, grey bars) and after 15 days of treatment (black bars) and 30 days of treatment (hatched bars), i.e. on D-4, D-2, D0, D13, D15, D17, D28, D30 and D32. Standard microbiological methods (based on selective media and culture conditions) were used to quantify counts of the potentially pathogenic bacteria Enterobacteriaceae (A) and *Enterococcus* spp. (B), and the beneficial bacteria *Lactobacillus* (D) and *Bifidobacterium* (C) in the colonic reactor R4. The data are expressed as the mean ± SD (n=3); ***p <0.001, **p <0.01, *p <0.05.

Figure 3: Short-chain fatty acid production in reactor 4 following treatment with CPF and/or inulin.

After 14 days of stabilization, the SHIME® was exposed to daily treatment with CPF (3.5 mg) and/or inulin (10 g). Three samples were collected every other day before treatment (D0, grey bars) and after 15 days of treatment (black bars) and 30 days of treatment (hatched bars), i.e. on D-4, D-2, D0, D13, D15, D17, D28, D30 and D32. Total SCFA levels were measured (D), together with the relative levels of acetate (A), propionate (B) and butyrate (C). The data are expressed as the mean ± SD (n=3); ***p <0.001, **p <0.01, *p <0.05.

Figure 4: IL-8 production by Caco-2/TC7 cells following exposure to SHIME® samples.

After 21 days of culture, caco-2/TC7 cells were exposed for 6 hours to samples collected from the SHIME® after 0, 15 or 30 days of CPF and inulin co-treatment. IL-8 production in the apical medium was measured by flow cytometry. The data are expressed as the mean ± SD (n=3); *p <0.05.

Tables

Table 1: pH values, working volumes, and residence times for the SHIME® reactors corresponding to each segment of the human intestinal tract.

Reactor	Segment modelled	pH	Working volume	Residence time
1	Stomach	2	200 ml	3 h
2	Duodenum/jejunum	7	300 ml	3 h
3	Ileum/cecum	7	300 ml	4 h
4	Ascending colon	5.5 – 6.0	1000 ml	20 h
5	Transverse colon	6.0 – 6.4	1600 ml	32 h
6	Descending colon	6.4 – 6.8	1200 ml	24 h

Adapted from (Joly et al. 2013)

Table 2: Relative expression levels of genes involved in the barrier function of intestinal epithelial cells, following exposure of Caco-2/TC7 cell monolayers to SHIME® samples.

After 6 h incubation with SHIME® extracts, cells were collected and the RNA was amplified to measure changes in the relative expression of target genes (n=3). The data are expressed as the mean ± SD (n=3); CPF: chlorpyrifos alone; INU: inulin alone; CPF+INU: co-treatment with CPF and inulin; significantly different ($p<0.05$) from D0 of CPF alone (*), D0 of INU alone (#), D15 of INU alone ($) D0 of CPF+INU (¤), D15 of CPF+INU (Δ).

Gene	Treatment	D0	D15	D30
ACTB	CPF	0.893±0.2885	0.694±0.0709	0.681±0.0530
	INU	1.086±0.6307	1.710±0.1697	0.936±0.1351
	CPF+INU	1.232±0.8975	1.107±0.3080	1.731±1.0741
CAV1	CPF	1.171±0.0148	0.642±0.0365*	0.777±0.1563
	INU	1.358±0.0516	1.308±0.3005	1.229±0.1655
	CPF+INU	1.116±0.1735	0.978±0.1578	0.916±0.1831
VIL1	CPF	0.997±0.0559	0.525±0.0666*	0.622±0.0092
	INU	1.346±0.2008	1.105±0.3465	1.083±0.0325
	CPF+INU	1.059±0.1068	1.223±0.2822	1.919±0.1082¤Δ
CDH1	CPF	0.919±0.0658	0.490±0.0560*	0.620±0.0354
	INU	1.505±0.0021	0.990±0.1662#	1.085±0.0665#
	CPF+INU	1.108±0.0695	1.169±0.2431	2.236±0.0750¤Δ
CLDN4	CPF	1.892±0.0375	1.141±0.1155*	1.408±0.8174
	INU	1.948±0.3224	0.621±0.1273#	1.119±0.0651#
	CPF+INU	1.039±0.2097	0.535±0.1161	0.662±0.2213
OCLN	CPF	0.736±0.0834	0.423±0.0235	0.528±0.0502
	INU	1.420±0.2079	1.377±0.3387	1.031±0.3161
	CPF+INU	0.955±0.2143	1.350±0.3880	3.706±1.4142¤Δ
TJP1	CPF	0.638±0.0997	0.346±0.0158	0.427±0.0071
	INU	1.830±0.3734	2.173±1.1971	1.143±0.6215
	CPF+INU	0.811±0.2806	1.383±0.5673	5.458±4.2349¤Δ
ALPI	CPF	1.104±1.0578	0.592±0.0651	1.639±2.0061
	INU	0.948±0.9065	4.511±2.1616#	0.711±0.7686$
	CPF+INU	0.824±0.2193	0.875±0.2839	4.375±0.2927¤Δ
SI	CPF	0.673±0.0820	0.675±0.4455	1.346±0.3578
	INU	1.154±0.1188	1.651±1.6263	2.515±2.4720
	CPF+INU	0.710±0.5580	0.814±0.3020	4.555±2.4558¤Δ

TLR4	CPF	0.594±0.3776	0.780±0.6941	0.568±0.1952
	INU	0.733±0.3479	2.989±1.3272	0.714±0.8266
	CPF+INU	0.828±0.8046	2.025±1.1580	8.731±1.3923¤Δ
TLR5	CPF	0.458±0.3543	0.175±0.0797	0.619±0.2913
	INU	3.099±0.9744	3.902±2.9748	1.526±1.5945
	CPF+INU	0.800±0.7584	3.372±1.8842	3.221±1.8368

Supplementary table 1: List of target genes and the corresponding primers

All sequences designed by PrimerDesign.

Target gene			Amplicon information	
Protein name	**Accession number**	**Gene symbol**	**Amplicon product length (bp)**	**Anchor nucleotide from the 3' end of the sequence**
Caveolin 1	NM_001753	*CAV1*	100	2265
Villin 1	NM_007127	*VIL1*	92	1528
Cadherin 1	NM_004360	*CDH1*	89	2331
Claudin 4	NM_001305	*CLDN4*	121	945
Occludin	NM_002538	*OCLN*	108	1107
Tight junction protein 1	NM_003257	*TJP1*	95	3554
Alkaline phosphatase, intestinal	NM_001631	*ALPI*	150	1386
Sucrase-isomaltase	NM_001041	*SI*	125	2250
Toll-like receptor 4	NM_138554	*TLR4*	98	1531
Toll-like receptor 5	NM_003268	*TLR5*	90	2090
Endogenous control glyceraldehyde 3-phosphate dehydrogenase	NM_002046	*GAPDH*	142	1087
ATP synthase	NM_001686	*ATP5B*	150	1200
Actin-beta	NM_001101	*ACTB*	106	1195

Supplementary Table 2: Trans-epithelial electric resistance of caco-2/TC7 monolayer during treatment.

Cells were incubated with DMEM cell culture medium or SHIME® extract for 24 hours (n=3). Trans-epithelial electrical resistance (in ohms) was measured throughout the incubation to check for integrity of the monolayer. The data are expressed as the mean ± SD (n=3); CPF: chlorpyrifos, INU: inulin, MIX: CPF and inulin. For each treatment, D0 is considered the reference medium for TEER measure.

* significantly different from (below) D0 (untreated) cells for the same condition.

Treatment	**T0**	T2	T4	T6	T8	T24
DMEM	**295.5 ± 7.09**	291.2 ± 8.35	293.8 ± 8.73	295.5 ± 14.94	287.7 ± 16.10	281.0 ± 14.25
CPF						
D0	**338.8 ± 16.41**	323.2 ± 18.46	303.2 ± 28.55	273.3 ± 15.89*	273.1 ± 32.52*	195.2 ± 14.15*
D15	323.2 ± 11.10	349.0 ± 12.83	330.1 ± 16.58	288.7 ± 32.08*	276.0 ± 28.00*	222.9 ± 20.20*
D30	319.8 ± 10.65	298.2 ± 21.06	285.2 ± 18.18*	266.3 ± 14.04*	253.5 ± 13.03*	191.0 ± 7.75*
INU						
D0	**364.7 ± 16.18**	312.2 ± 19.73*	293.1 ± 7.82*	261.2 ± 16.60*	250.9 ± 21.89*	195.7 ± 14.85*
D15	388.3 ± 35.90	274.3 ± 21.25*	284.6 ± 14.87*	261.4 ± 14.34*	225.7 ± 13.79*	222.0 ± 27.41*
D30	380.0 ± 23.96	337.0 ± 15.32	293.9 ± 21.68*	291.9 ± 29.28*	277.4 ± 24.98*	191.0 ± 7.75*
MIX						
D0	**306.9 ± 11.21**	280.3 ± 10.79	275.1 ± 10.03*	273.2 ± 9.98*	236.4 ± 10.77*	191.0 ± 7.75*
D15	329.6 ± 32.19	280.8 ± 18.21	284.1 ± 21.54	283.9 ± 16.09	265.1 ± 28.52*	211.8 ± 36.52*
D30	314.0 ± 13.55	285.1 ± 17.01	271.0 ± 7.92*	257.6 ± 16.78*	231.6 ± 10.99*	175.2 ± 6.26*

Supplementary Table 3: Relative expression levels of genes involved in the barrier function of intestinal epithelial cells, following exposure of Caco-2/TC7 cell monolayers to CPF samples.

After 24 h incubation with CPF, cells were collected and the RNA was amplified to measure changes in the relative expression of target genes (n=4). The data are expressed as the mean ± SD (n=4); CPF: chlorpyrifos significantly different from CPF-free control (*).

Gene	CPF-0	CPF-250µM	CPF-500µM
ACTB	1.0835	1.072	1.0835
CAV1	0.762	1.225	1.449
VIL1	0.761	1.225	1.2085
CDH1	0.7965	0.8895	1.22
CLDN4	0.793	1.5305	1.10025
OCLN	0.6945	0.89925	1.05025
TJP1	0.8055	1.03775	1.43725
ALPI	0.8635	0.807	0.8455
SI	0.8935	0.84675	1.00325

Figures

Figure 1

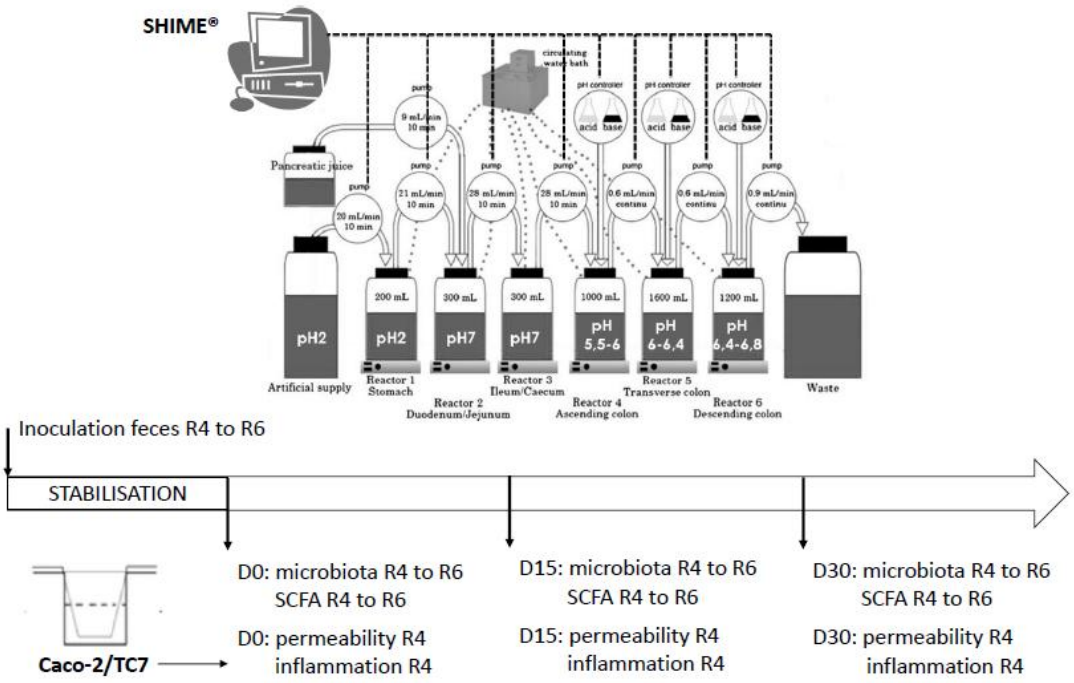

Figure 2:

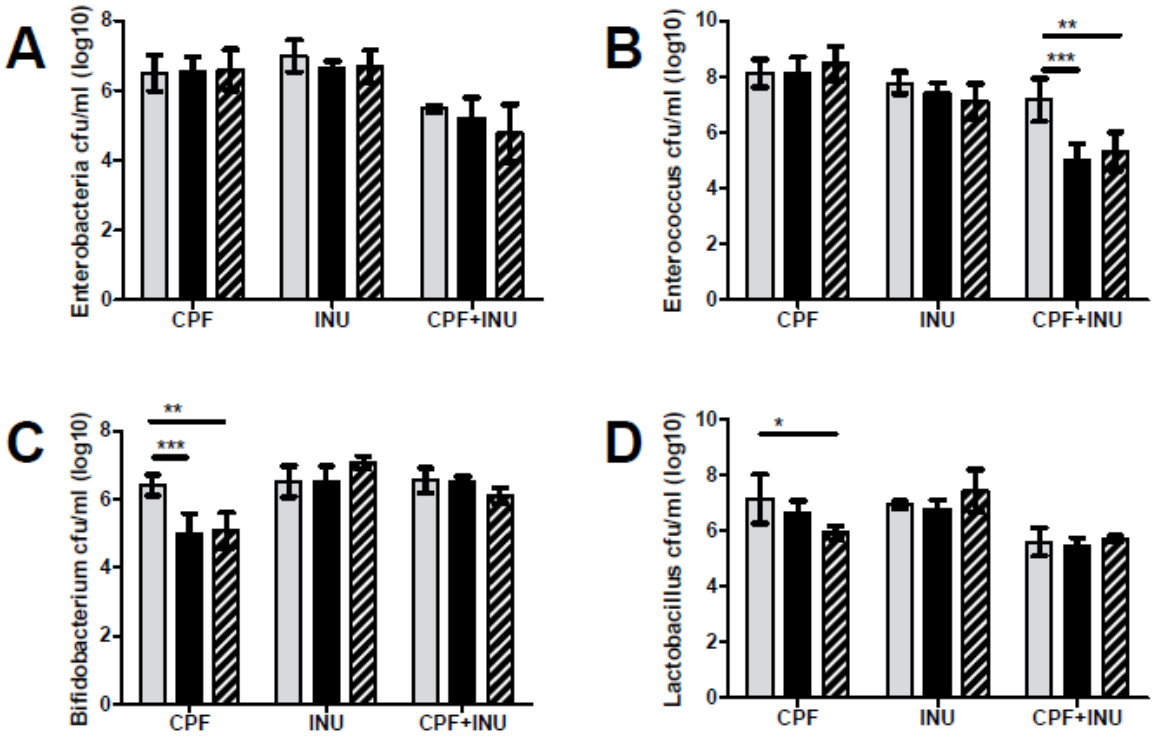
A
Enterobacteria cfu/ml (log10)
0
2
4
6
8
CPF
INU
CPF+INU
B
Enterococcus cfu/ml (log10)
0
2
4
6
8
10
**
***
CPF
INU
CPF+INU
C
Bifidobacterium cfu/ml (log10)
0
2
4
6
8
**
***
CPF
INU
CPF+INU
D
Lactobacillus cfu/ml (log10)
0
2
4
6
8
10
*
CPF
INU
CPF+INU

Figure 3

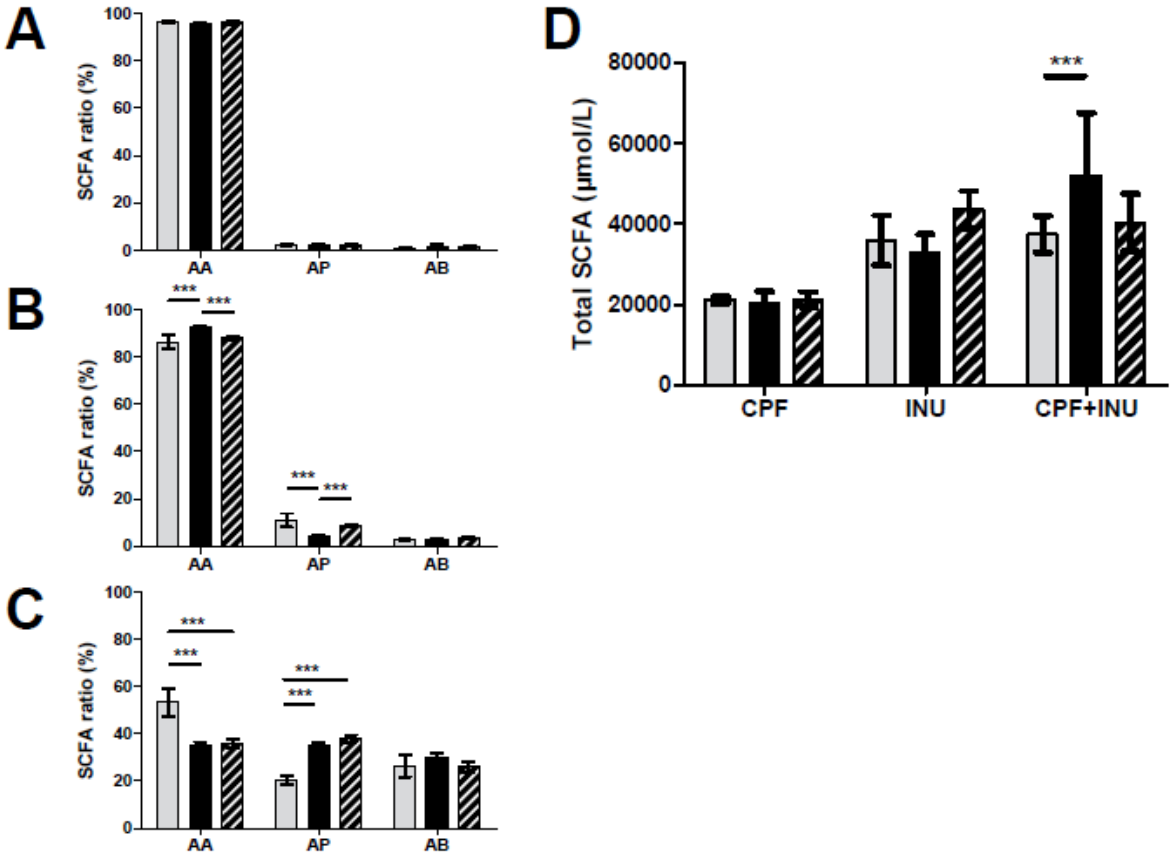

Figure 4:

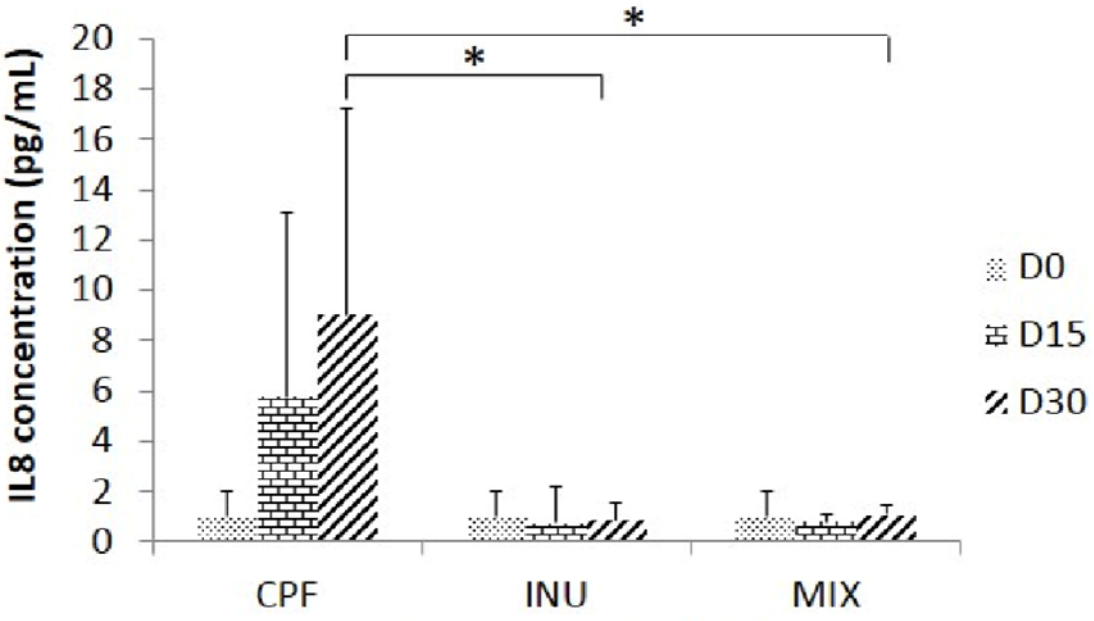
IL8 concentration (pg/mL)
20
18
16
14
12
10
8
6
4
2
0
*
*
CPF
INU
MIX
D0
D15
D30